

# AqF026 Is a Pharmacologic Agonist of the Water Channel Aquaporin-1

Andrea J. Yool,\* Johann Morelle,<sup>†</sup> Yvette Cnops,<sup>†</sup> Jean-Marc Verbavatz,<sup>‡</sup> Ewan M. Campbell,\* Elizabeth A.H. Beckett,\* Grant W. Booker,<sup>§</sup> Gary Flynn,<sup>||</sup> and Olivier Devuyst<sup>†||</sup>

\*School of Medical Sciences and the Adelaide Centre for Neuroscience Research and <sup>§</sup>School of Molecular & Biomedical Sciences, University of Adelaide, Adelaide, South Australia, Australia; <sup>†</sup>Division of Nephrology, Université catholique de Louvain Medical School, Brussels, Belgium; <sup>‡</sup>Max Planck Institute of Molecular Cell Biology and Genetics, Dresden, Germany; <sup>||</sup>Spacefill Enterprises LLC, Tucson, Arizona; and <sup>†||</sup>Institute of Physiology, Zurich Centre for Integrative Human Physiology, University of Zurich, Zurich, Switzerland

## ABSTRACT

Aquaporin-1 (AQP1) facilitates the osmotic transport of water across the capillary endothelium, among other cell types, and thereby has a substantial role in ultrafiltration during peritoneal dialysis. At present, pharmacologic agents that enhance AQP1-mediated water transport, which would be expected to increase the efficiency of peritoneal dialysis, are not available. Here, we describe AqF026, an aquaporin agonist that is a chemical derivative of the arylsulfonamide compound furosemide. In the *Xenopus laevis* oocyte system, extracellular AqF026 potentiated the channel activity of human AQP1 by >20% but had no effect on channel activity of AQP4. We found that the intracellular binding site for AQP1 involves loop D, a region associated with channel gating. In a mouse model of peritoneal dialysis, AqF026 enhanced the osmotic transport of water across the peritoneal membrane but did not affect the osmotic gradient, the transport of small solutes, or the localization and expression of AQP1 on the plasma membrane. Furthermore, AqF026 did not potentiate water transport in *Aqp1*-null mice, suggesting that indirect mechanisms involving other channels or transporters were unlikely. Last, in a mouse gastric antrum preparation, AqF026 did not affect the Na-K-Cl cotransporter NKCC1. In summary, AqF026 directly and specifically potentiates AQP1-mediated water transport, suggesting that it deserves additional investigation for applications such as peritoneal dialysis or clinical situations associated with defective water handling.

J Am Soc Nephrol 24: 1045–1052, 2013. doi: 10.1681/ASN.2012080869

Aquaporin-1 (AQP1) is the archetypal member of a family of membrane water channels that is conserved in mammals, microorganisms, and plants.<sup>1</sup> Mammalian aquaporins (AQPs) are distributed in specific cell types in numerous tissues and organs, where they facilitate the osmotic transport of water and regulate body fluid homeostasis. Most AQPs are constitutively expressed in plasma membranes, where they exist as homotetramers. Each monomer has six membrane-spanning domains and two

short hydrophobic loops containing conserved motifs and residues that are critical for the water selectivity of the pore.<sup>2</sup> AQP1 is abundantly expressed in the endothelium-lining nonfenestrated capillaries located in the kidney, the airways, and the pleural and peritoneal membranes.<sup>3,4</sup> In the kidney, AQP1 mediates the water transport across the vasa recta, which influences the medullary blood flow and urinary concentrating ability. A significant urinary-concentrating defect is observed in both

*Aqp1*-null mice and humans deficient in AQP1.<sup>5,6</sup>

The development of pharmacologic agents able to modulate AQPs has been a highly anticipated goal, stimulated by insights in aquaporin structure and functional regulation.<sup>7</sup> As a proof of concept, induction of AQP1 transcription in endothelial cells by corticosteroids is associated with an increase in water transport *in vivo*.<sup>8</sup> Antagonists for AQP1 and AQP4 have been developed, with a focus on arylsulfonamide compounds, including acetazolamide,<sup>9</sup> antiepileptic agents,<sup>10</sup> and derivatives of the loop diuretic bumetanide.<sup>11</sup> However, the effectiveness of acetazolamide and antiepileptics as AQP blockers has been disputed.<sup>12</sup> The bumetanide derivative AqB013 (Aq, aquaporin ligand; B, bumetanide scaffold) at 20  $\mu$ M blocks AQP1 and AQP4 by a mechanism

Received August 29, 2012. Accepted March 7, 2013.

Published online ahead of print. Publication date available at www.jasn.org.

**Correspondence:** Dr. Olivier Devuyst, Institute of Physiology, University of Zurich, Winterthurerstrasse 190, CH 8057 Zurich, Switzerland, or Dr. Andrea J. Yool, School of Medical Sciences, University of Adelaide, Medical School South level 4, Frome Road, Adelaide SA 5005, Australia. Email: olivier.devuyst@uzh.ch or andrea.yool@adelaide.edu.au

Copyright © 2013 by the American Society of Nephrology

thought to involve physical occlusion of the intracellular water channel pore.<sup>11</sup> No direct pharmacologic agonist of AQPs has previously been described.

The functional relevance of AQP1 is particularly evident when osmotic water transport during peritoneal dialysis is considered.<sup>13</sup> Peritoneal dialysis is based on diffusive and convective transport of solutes and water between peritoneal capillaries and a dialysis solution present in the peritoneal cavity. The capacity to remove water in excess across the peritoneal membrane (ultrafiltration) is a major predictor of outcome and mortality for patients treated by this modality.<sup>14</sup> Detailed studies in *Aqp1*-null mice have demonstrated that AQP1 water channels correspond to water-specific pores located in peritoneal capillaries,<sup>15,16</sup> which represent the major transport barrier of the membrane.<sup>17</sup> An agonist of AQP1 would be expected to enhance water transport and ultrafiltration, thereby increasing the efficiency of dialysis.<sup>8,13</sup> Furthermore, because peritoneal dialysis allows the specific assessment of AQP1-mediated water transport, as opposed to effects on small solute transport and osmotic gradient, it is an advantageous model for assessing potential modulators of AQP1 *in vivo*.

In the present study, we tested the capacity of the novel agent AqF026 (Aq, aquaporin ligand; F, furosemide scaffold) to potentiate the water channel activity of AQP1 *in vitro* and *in vivo*. Rates of net water flux were measured in control and AQP1-expressing *Xenopus laevis* oocytes preincubated with and without externally applied AqF026 (Figure 1). Increases in relative volume as a function of time in hypotonic saline (Figure 1A) yielded slope values (relative swelling rates, Figure 1B) that showed a maximal potentiation at 5  $\mu\text{M}$  for AQP1, and loss of the agonist effect at AqF026 doses  $\geq 100 \mu\text{M}$ . Dose-response curves (Figure 1C) indicated an estimated half maximal effective concentration ( $\text{EC}_{50}$ ) value of 3.3  $\mu\text{M}$  for AQP1. AqF026 also potentiated the closely related AQP4, but with substantially reduced efficacy. AQP4-mediated water transport increased significantly only at  $\geq 50 \mu\text{M}$

AqF026 (Figure 1, B and C). These results suggest a relatively high specificity for the potentiating effect, in that AqF026 distinguished between two aquaporins, AQP1 and AQP4, with  $>40\%$  identity and 60% homology in amino acid sequence (based on GenBank Clustal analysis).

Using available crystal structure data, theoretical docking supported a direct interaction of AqF026 at a site located at the intracellular side of AQP1 (Figure 2A). The chemically distinguishing feature of AqF026 compared with the parent compound furosemide is an aromatic ring linked to the sulfonamide moiety (Figure 2B). *In silico* modeling suggested the binding of AqF026 involved residues in the loop D domain as well as other intracellular domain residues in the vicinity (Figure 2C). Theoretical ligand docking suggested that the distinctive sulfhydryl-linked aromatic ring of AqF026 interacted with arginine 159 in human AQP1 (Arg 161 in bovine AQP1). Of note (Supplemental Table 1), the equivalently positioned residue in AQP4 loop D is serine 180, the proposed site of water channel regulation by phosphorylation.<sup>18</sup> A second residue implicated in the putative AqF026-binding site in human AQP1 is threonine 157 (bovine Thr 159). The equivalent cysteine residue at position 178 in AQP4 loop D confers sensitivity to block by intracellularly applied mercurial compounds.<sup>19</sup> The functional roles of AQP4 loop D residues support the proposal that the loop D region is an important regulatory domain, and the observed differences between AQP1 and AQP4 at key amino acid positions could contribute to the difference in efficacy of AqF026 (Figure 1). Site-directed mutagenesis of intracellular residues in the AQP1 loop D domain that were modeled as being involved in ligand docking (Figure 2, D and E) showed that the agonist effect of AqF026 could be reversed by mutations of threonine 157 or arginine 159 and 160. Conversely, mutation of glycine 165, a loop D residue not implicated in the candidate binding site, did not prevent the agonist activity of AqF026. The magnitude of agonist potentiation with

Gly165Pro was not significantly different from that seen with AqF026-treated wild type AQP1. A significant increase in osmotic water permeability over control levels demonstrated the functional expression of the AQP1 wild type and mutant constructs in the oocyte plasma membrane, a finding that was confirmed by immunocytochemical labeling and confocal imaging of whole oocytes (Figure 2E). Taken together, these data demonstrate that AqF026 causes a dose-dependent potentiation of human AQP1 water channel activity and that the effect is likely to be mediated by ligand binding at an intracellular site involving specific amino acid residues in the loop D and possibly other adjacent intracellular domains.

To determine whether AqF026 retained any Na-K-Cl cotransporter (NKCC) blocking activity that is a hallmark feature of the parent compound furosemide, we took advantage of a mouse gastrointestinal smooth muscle preparation as sensitive bioassay for NKCC activity (Figure 2F). The mammalian gastrointestinal tract has pacemaker-driven slow-wave electrical activity, thought to be mediated by  $\text{Ca}^{2+}$ -activated chloride channels.<sup>20</sup> The maintenance of a negative baseline membrane potential is critically dependent on the function of NKCC1. Block of NKCC1 in mouse intestine with bumetanide (4  $\mu\text{M}$ ) produced a reversible 10-mV depolarization of the baseline membrane potential that was not seen in NKCC1 knockout mice.<sup>21</sup> Similar, reversible depolarizations were induced by bumetanide or by furosemide in the guinea pig gastric antrum.<sup>22</sup> We found that the classic slow-wave pattern in mouse gastric antrum similarly was altered within 10 minutes after application of a methylated furosemide agent (10  $\mu\text{M}$  AqF022). The effect was reversed by washout, and AqF026 at the same dose had no discernable effect on membrane potential or slow wave signaling over 30 minutes (Figure 2F), indicating that the addition of the sulfonamide aryl group abolished any appreciable effect on NKCC1 while endowing AQP1 agonist activity. These results are consistent with structural

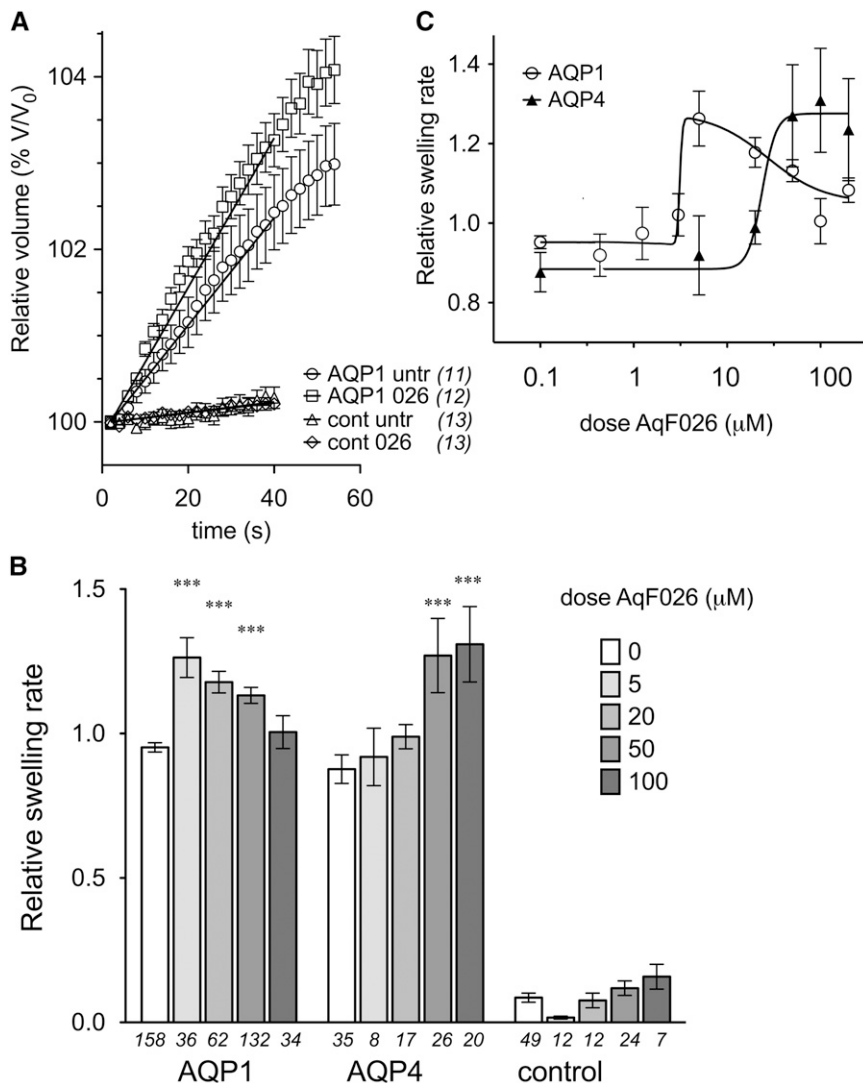


**Figure 1.** Potentiating effect of AqF026 on water channel activity of AQP1 and AQP4 expressed in *Xenopus laevis* oocytes. (A) Change in volume ( $V$ ) due to osmotic swelling, standardized to the initial volume ( $V_0$ ) and plotted as a function of time in 50% hypotonic saline, for AQP1-expressing and -nonexpressing control (cont) oocytes. Oocytes were preincubated in 10  $\mu\text{M}$  AqF026 or with DMSO alone (untr) as a vehicle control. Data are mean  $\pm$  SEM for all oocytes tested in a single experimental day;  $n$  values are indicated in italics. (B) Histogram of compiled data showing maximal potentiation of AQP1 near 5  $\mu\text{M}$  AqF026 and no potentiation of AQP4 at doses  $<50$   $\mu\text{M}$ . (C) Dose-response relationships for AqF026-mediated potentiation of AQP1 and AQP4 water channel activities, with an estimated  $\text{EC}_{50}$  value of 3.3  $\mu\text{M}$  and a Hill coefficient of 1.8 for the stimulatory component for AQP1 (fit as the sum of two dose-response curves, one stimulatory and one inhibitory, using GraphPad Prism).

modeling data indicating that the introduced aromatic ring appears to be key in the ligand interaction with loop D. Furthermore, the lack of effect of AqF026 on any properties of slow-wave signaling further supports the idea that this agent is unlikely to have indirect effects on

general membrane properties or the broad array of channels and transporters also present in this preparation.

We used an established mouse model of peritoneal dialysis<sup>16,23</sup> to test the relevance of the agonist activity of AqF026 on water transport and ultrafiltration *in*

*in vivo* (Figure 3). Treatment of wild-type mice with AqF026 resulted in an approximately 15% increase in fluid transport across the peritoneal membrane (Figure 3A and Table 1), similar to the potentiation of AQP1 seen at 5–20  $\mu\text{M}$  *in vitro*. The effect of AqF026 was dose dependent, with a maximal response observed for a concentration of 15  $\mu\text{M}$  (Figure 3A) and an  $\text{EC}_{50}$  value of 4.2  $\mu\text{M}$  (Figure 3A, inset). The effect of AqF026 on net ultrafiltration and initial ultrafiltration rate was maximal at about 120 minutes after injection (Figure 3B), in agreement with *in vitro* studies. The ultrafiltration in AQP1-null mice was 60% lower than in their wild-type littermates, and this measure was not affected by AqF026 administration (Figure 3A). The agonist effect of AqF026 on osmotic water transport was further demonstrated by increased intraperitoneal volume curve over time (Figure 3C) and an approximately 50% increase in the initial ultrafiltration rate across the peritoneal membrane (Figure 3D;  $32.2 \pm 1.3$   $\mu\text{l}/\text{min}$  versus  $21.9 \pm 0.8$   $\mu\text{l}/\text{min}$ , in AqF026 versus vehicle-treated *Aqp1*<sup>+/+</sup> mice, respectively;  $P < 0.001$ ). In contrast, treatment with AqF026 had no effect on the initial ultrafiltration rate in the *Aqp1*-null mice (Figure 3D).

The decrease in dialysate sodium concentration during the initial phase of a hypertonic dwell (“sodium sieving”) is a reliable index of AQP1-mediated water transport in PD.<sup>16,17</sup> Administration of AqF026 was also reflected by a significant increase in that variable (dip in sodium dialysate within the first 30 minutes of the dwell:  $11.2 \pm 0.3$  mEq/l versus  $8.9 \pm 0.9$  mEq/l in AqF026-treated versus vehicle-treated mice,  $n = 10$  pairs,  $P = 0.03$ ) (Figure 3E). Administration of AqF026 had no detectable effects on the osmotic gradient (Figure 3F and Table 1), small solute transport as measured for urea and glucose (Figure 3, G and H, and Table 1), and rate of albumin leakage in the dialysate (dialysis to plasma ratio albumin:  $0.09 \pm 0.005$  versus  $0.10 \pm 0.003$  in AqF026-treated versus vehicle-treated mice,  $n = 6$  pairs).

No differences in urine output, hemolysis (lactate dehydrogenase), or liver toxicity (aspartate aminotransferase and

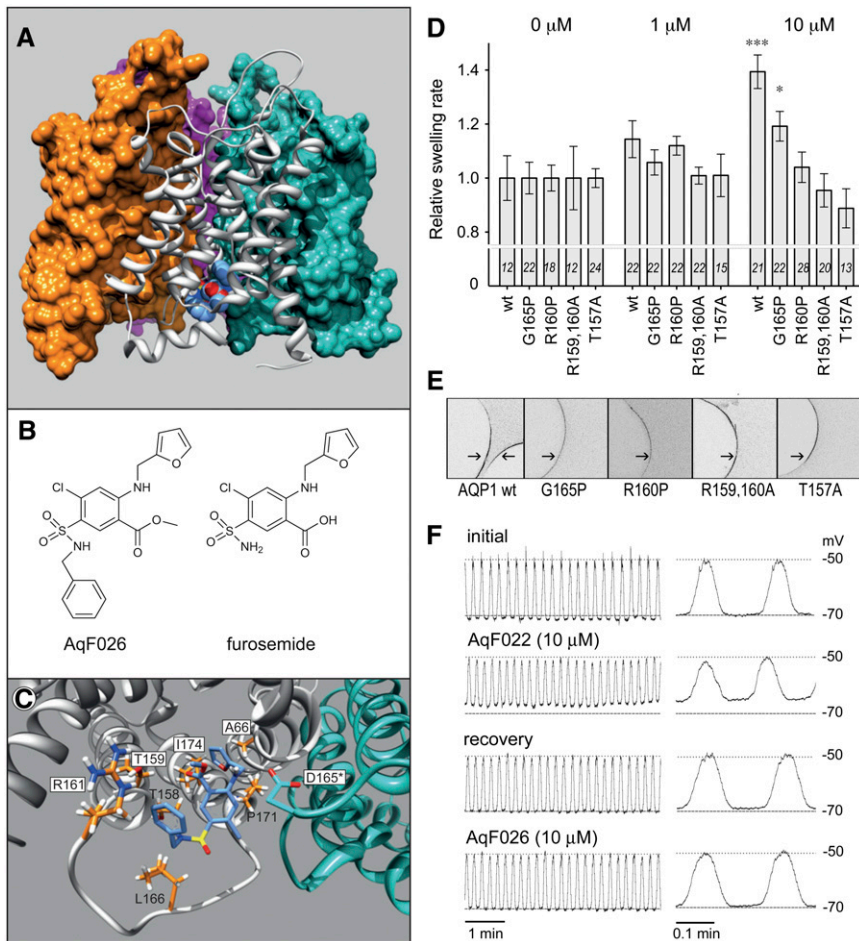


**Figure 2.** Ligand docking of AqF026 on AQP1: involvement of loop D domain residues and specificity of action using an NKCC1-sensitive bioassay. The identification of residues associated with the proposed intracellular binding pocket are based on the crystal structure of bovine AQP1. (A) Surface rendition of the tetramer with the docked pose of AqF026 in a ribbon structure of one AQP1 subunit. (B) Chemical structure of AqF026 and the parent compound furosemide. (C) A detailed view of the amino acid side chains relevant to the docked pose. The highlighted residue (D165\*) indicates an amino acid contribution from a neighboring subunit. (D) Relative swelling rates were standardized to the untreated AQP1 wild-type or mutant channel responses within the same batches of oocytes, and data were compiled from at least three different batches for each group. Data are mean  $\pm$  SEM; *n* values are shown in italics above the x axis. Asterisks indicate a significantly different effect for the comparison of 0 and 10  $\mu\text{M}$  AqF026 for the same construct (\* $P < 0.05$ ; \*\*\* $P < 0.001$ ). There was no significant difference between wild type and G165P at 10  $\mu\text{M}$  (not indicated). (E) Confocal images of permeabilized immunolabeled oocytes expressing AQP1 wild-type or mutants, showing channel protein localization in plasma membranes (arrows). (F) Intracellular recording from a mouse gastric antrum preparation, continuously measured from a single circular smooth muscle cell. Traces show representative segments from the sequence: first confirming stable spontaneous slow-wave activity (initial); after treatment with a methylated furosemide compound (AqF022, 10  $\mu\text{M}$ ), which caused depolarization and a concomitant decline in slow-wave amplitude; after reversal of the effect by washout (recovery); and during the subsequent lack of effect of AqF026 (10  $\mu\text{M}$ ) over an extended period (30 minutes). Similar results were seen in three replicate cells.

alanine aminotransferase) variables were observed in mice exposed to AqF026 versus vehicle during the PD exchange

(data not shown). Treatment with AqF026 did not appreciably change the levels of protein or mRNA expression of

AQP1 in the peritoneum (Supplemental Figure 1, A–C). Immunogold electron microscopy showed that the distribution and abundance of AQP1 were not visibly different in wild-type mice treated with vehicle and AqF026 (density of AQP1-gold particles:  $5.08 \pm 1.06$  versus  $5.78 \pm 0.63$  particles/ $\mu\text{m}^2$ , respectively;  $n = 7$  pairs) (Supplemental Figure 1D).

Results here are the first to define a pharmacologic ligand that potentiates AQP1 water channel activity, to show that it is effective *in vitro* and *in vivo*, and to identify a candidate molecular site of action. The data are consistent with direct binding of the novel arylsulfonamide compound AqF026 at a site involving the intracellular regulatory domain loop D in AQP1. The specificity of the drug on AQP1 is substantiated by several lines of evidence, obtained both *in vitro* and *in vivo*. First, AQP1 is much more sensitive to AqF026 than the closely related AQP4. Second, AqF026 has no effect on NKCC1 and no detectable diuretic effect during the peritoneal dialysis dwell. Third, AqF026 induces a strong increase in the initial ultrafiltration rate, reflecting the essential contribution of AQP1 to transcapillary ultrafiltration at this stage. The effect is abolished when AqF026 is administered to *Aqp1*-null mice. Fourth, the administration of AqF026 is reflected by an increase in the sodium sieving, which typically reflects the movement of free water through AQP1. Finally, the lack of effect of AqF026 on other compartments can be inferred by the unchanged transport of small solutes and the lack of structural changes in the membrane.

Modulators of AQP1 with translational potential have been slow to emerge. Blockers have only been described thus far, limited by toxicity, low efficacy, and lack of specificity.<sup>24</sup> Arylsulfonamide compounds, including carbonic anhydrase inhibitors, appeared as potentially attractive candidates on the basis of efficacy and safety index.<sup>9,10</sup> Of particular interest, a 4-aminopyridine carboxamide derivative of the loop diuretic bumetanide (AqB013) was shown to inhibit AQP1 *in vitro* (50% inhibitory concentration, approximately 20  $\mu\text{M}$ , extracellularly) by

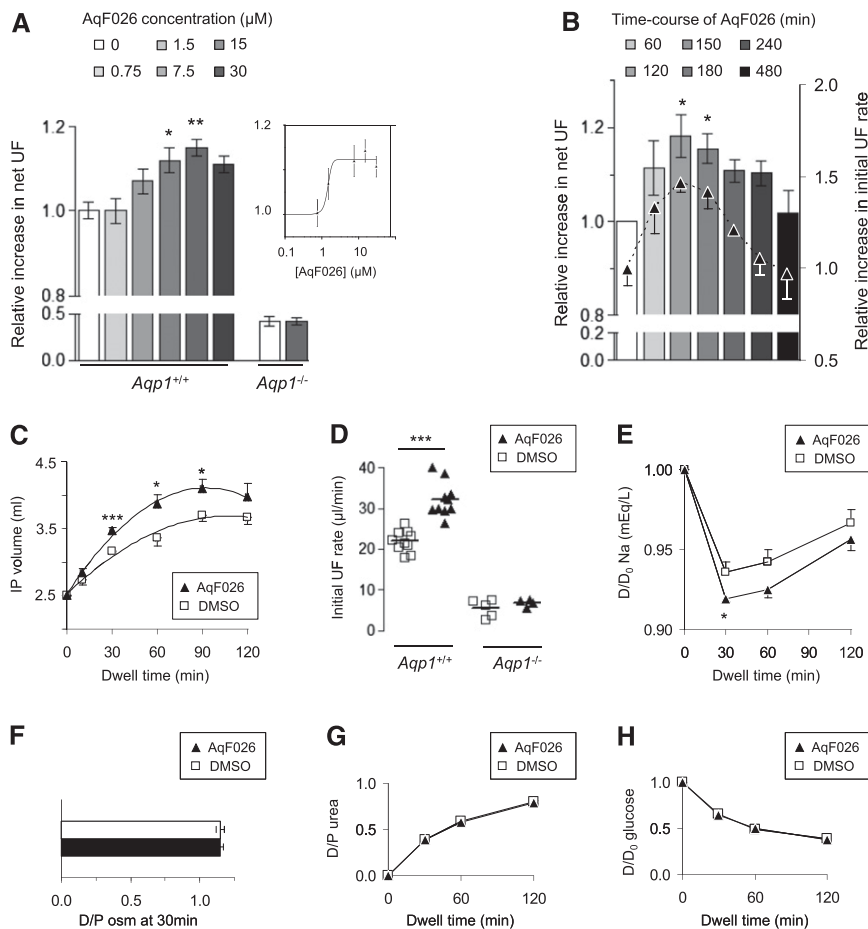


**Figure 3.** AqF026 specifically enhances AQP1-mediated osmotic water transport *in vivo*. (A) Wild-type  $Aqp1^{+/+}$  mice treated with AqF026 have a significant, dose-dependent increase in net ultrafiltration (UF) across the peritoneal membrane. The maximal response is observed for a concentration of 15  $\mu\text{M}$ , with an estimated  $\text{EC}_{50}$  value of 4.2  $\mu\text{M}$  (inset).  $Aqp1^{-/-}$  mice, characterized by a 60% reduction in ultrafiltration at baseline, show no potentiation of the ultrafiltration after treatment with 15  $\mu\text{M}$  AqF026. Data are mean  $\pm$  SEM;  $n=6$  for each AqF026 concentration except for 0.75  $\mu\text{M}$  ( $n=4$ ). Net ultrafiltration rates were standardized to body weight and compared with rates in vehicle-treated mice (open bar). (B) Time course performed in wild-type mice shows that the effect of AqF026 (15  $\mu\text{M}$ ) on net ultrafiltration (bars) and initial ultrafiltration rate (triangles) is maximal 120–150 minutes after intravenous injection. Data are mean  $\pm$  SEM;  $n=4$  for each time point. Open bar corresponds to vehicle-treated mice. (C) Treatment of  $Aqp1^{+/+}$  mice with 15  $\mu\text{M}$  AqF026 results in increased intraperitoneal (IP) volume over time ( $P=0.02$  between the AqF026 and vehicle curves), with significant differences at 30, 60, and 90 minutes in AqF026-treated (black triangles) compared with vehicle-treated (open squares) animals ( $P<0.01$ ,  $P<0.05$ , and  $P<0.05$  respectively;  $n=10$  in each group). (D) Initial ultrafiltration rates, taken as an index of AQP1-mediated water transport during the first part of the dwell, are significantly increased in  $Aqp1^{+/+}$  mice treated with 15  $\mu\text{M}$  AqF026 versus vehicle ( $P<0.001$ ,  $n=10$  in each group). In contrast, AqF026 has no effect on the initial ultrafiltration rates in  $Aqp1^{-/-}$  mice (AqF026,  $n=4$  and vehicle-treated,  $n=5$ ). (E) Treatment of wild-type mice with AqF026 (15  $\mu\text{M}$ ) induces a significant increase in sodium sieving ( $D/D_0$  sodium at 30 min) compared with vehicle-treated animals ( $P<0.05$ ;  $n=10$  in each group). (F–H) The dialysate-to-plasma ratio of osmolality at 30 minutes (D/P osm) (F), the dialysate-to-plasma ratio of urea (D/P urea) (G), and the progressive removal of glucose from the dialysate ( $D/D_0$  glucose) (H) were similar in mice treated with 15  $\mu\text{M}$  AqF026 versus vehicle ( $n=12$  pairs of  $Aqp1^{+/+}$  mice).

acting at an intracellular side that occludes the water pore.<sup>11</sup>

In this study, we used another loop diuretic, furosemide, as a scaffold for the creation of the novel arylsulfonamide derivative, AqF026. Furosemide is relatively membrane impermeable, and it lacks a discernable effect on AQP1 or AQP4 water channel activity when applied extracellularly.<sup>11</sup> For the agonist AqF026, a furan-containing arylsulfonamide, the carboxylic acid of the furosemide scaffold was modified by conversion of its carboxylic acid group to a methyl ester and by addition of a benzyl group to the sulfonamide nitrogen. These modifications increased the calculated logP (logarithm of the oil:water partition coefficient, P) value to 2.97, a range that is consistent with drug-like properties.<sup>25</sup> An intracellular site of action of AqF026 on AQP1 channels was supported by the >1-hour latency for the agonist effect in the *Xenopus* system. Accumulating evidence suggests that AQPs are subject to complex mechanisms of regulation.<sup>26,27</sup> According to results of *in silico* modeling and mutagenesis, the added benzyl moiety appears to enable an interaction between the AqF026 ligand and residues in the proximal region of the loop D domain, within a zone that is increasingly investigated for AQP channel regulation.<sup>28–30</sup> In turn, such interaction could open the pore to increase unitary flux rates, remove a barrier or increase the probability of the open state.

The molecular mechanism for the biphasic action of AqF026 on AQP1 is not known. A testable hypothesis is that, at higher doses, the antagonistic effect might involve occlusion of the AQP1 water pore at the intracellular face at a site similar to that implicated for block by AqB013,<sup>11</sup> whereas the agonist effect at lower doses appears to result from regulation of channel activity at a separate allosteric site involving loop D. Alternatively, AqF026 could have different effects at the same site depending on concentration.

Studies on *Aqp1* knockout mice have demonstrated that AQP1 facilitates the osmotic water transport across the peritoneal membrane.<sup>15</sup> The fact that AqF026

**Table 1.** Effect of AqF026 on water and small solute transport *in vivo*

Group	Net UF/BW ( $\mu\text{l/g}$ )	D/P <sub>osm</sub> at 30 min	MTAC urea ( $\mu\text{l/min}$ )
Aqp1 <sup>+/+</sup> DMSO	37.2 $\pm$ 1.3	1.14 $\pm$ 0.03	35.0 $\pm$ 2.3
Aqp1 <sup>+/+</sup> AqF026	42.8 $\pm$ 1.4 <sup>a</sup>	1.15 $\pm$ 0.03	34.2 $\pm$ 1.7
Aqp1 <sup>-/-</sup> DMSO	15.7 $\pm$ 1.9 <sup>b</sup>	1.28 $\pm$ 0.02	35.5 $\pm$ 3.6
Aqp1 <sup>-/-</sup> AqF026	15.6 $\pm$ 1.6 <sup>b</sup>	1.27 $\pm$ 0.03	36.4 $\pm$ 7.0

Ultrafiltration and small solutes transport were measured in 16 pairs of Aqp1<sup>+/+</sup> mice and 6 pairs of Aqp1<sup>-/-</sup> mice. Osmolality was assessed in 12 pairs of Aqp1<sup>+/+</sup> mice and 6 pairs of Aqp1<sup>-/-</sup> mice. UF, ultrafiltration; BW, body weight; D/P<sub>osm</sub>, dialysate-over-plasma osmolality; MTAC, mass transfer area coefficient (calculated from Waniewski equation,  $f=0.33$ ).

<sup>a</sup> $P<0.05$  AqF026 versus DMSO.

<sup>b</sup> $P<0.001$  versus Aqp1<sup>+/+</sup>.

increased water transport and ultrafiltration *in vivo* in this model, without detectable changes in small solute transport or modifications of the expression of AQP1, suggests this agent has translational potential for patients treated with peritoneal dialysis. As expected, the maximal potentiation of AQP1-mediated free-water transport occurs during the first part of the dwell, when the osmotic gradient is maximal. In agreement with previous studies addressing free-water transport in rat and mouse models<sup>8,16</sup> and simulations based on the three-pore model (B. Rippe, unpublished data), the effect of AqF026 on free-water transport was observed in the absence of any detectable change in small solute transport.

ESRD is a major global concern, and improved methods for delivering replacement therapy *via* peritoneal dialysis would be of substantial significance. The use of AQP1 agonists in patients undergoing peritoneal dialysis would be of prime interest in patients developing ultrafiltration failure, who may show water channel dysfunction alone or combined with enlarged vascular surface area and/or increased lymphatic absorption rate.<sup>31</sup> By extension, a pharmacologic agonist of AQP1 might be useful in conditions associated with defective local water handling, including subretinal edema, neurodegenerative conditions and hydrocephaly, acute renal failure, and diabetes insipidus.

Because AqF026 is an agonist of AQP1 channels that are expressed in multiple organs, additional work on drug metabolism and potential toxicity will be important to evaluate potentially harmful effects. Loop diuretics are among the

most widely used drugs worldwide, with a well established safety index during acute or chronic administration.<sup>32</sup> Our cumulative observations with arylsulfonamide compounds AqB013 and AqF026 in rodents suggest these derivatives are well tolerated and cause no appreciable overt tissue or organ toxicity under the specific conditions tested thus far.

The identification of the first pharmacologic agonist for AQP1 opens new avenues for analyses of AQP1-mediated water transport and has potential therapeutic value for clinical situations based on osmotic water transport, including peritoneal dialysis.

## CONCISE METHODS

### *In Vitro* Assays

Expression of human AQP1 and rat AQP4 in *X. laevis* oocytes was done as described previously.<sup>30</sup> Site-directed mutations in AQP1 were generated by PCR using the QuikChange kit (Agilent Technologies, Australia). Non-AQP1-expressing control oocytes without cRNA injection were prepared from the same batches of oocytes. Responses were standardized to the mean swelling rate of the wild-type AQP1 untreated oocytes in the same batch of oocytes and compiled for multiple batches. All animal procedures were approved by the University of Adelaide Animal Ethics committee and performed in accord with the Australian Code of Practice for the Care and Use of Animals for Scientific Purposes.

### *In Silico* Modeling

The coordinates for the tetrameric model based on the crystal structure of bovine AQP1

were obtained from the Protein Data Bank (MMDB ID: 18789; PDB ID: 1J4N). The pdb file coordinates were prepared for docking by removing water molecules and adding charges using autodocktools-1.5.4. The coordinate files for the ligand molecules were obtained using Corina accessed *via* the National Cancer Institute's on-line SMILES translation tool and prepared for docking using autodocktools. The docking was performed using Autodock Vina<sup>33</sup> with a grid size of (80Å  $\times$  80 Å  $\times$  42Å) covering the entire cytoplasmic face of the tetramer. The highest ranked pose was used in the analysis.

### AqF026 Synthesis and Application

AqF026 was prepared by following a two-step process, in which furosemide was first converted to its methyl ester derivative (AqF022); then, alkylation of the sulfonamide ester yielded AqF026 (Supplemental Figure 2). Agents were purified by column chromatography. For *in vitro* assays of swelling, oocytes were incubated in isotonic Na<sup>+</sup> bath saline with AqF026 or DMSO vehicle before swelling assays. For *in vivo* studies, AqF026 or DMSO (vehicle control) diluted in sterile 0.9% NaCl was injected in the tail veins of mice at 30 minutes before the start of the experimental transport measurements.

### Mouse Gastric Antrum Electrophysiology

By following published methods,<sup>34</sup> adult Balb/C mice were anesthetized with isoflurane inhalation and euthanized by cervical dislocation. The stomach antral region (approximately 40 mm<sup>2</sup>) with the mucosa removed was pinned into a recording chamber lined with Sylgard elastomer (Dow Corning), and maintained in 37°C Krebs solution (in mM: NaCl 118, KCl 4.75, MgSO<sub>4</sub> 1.2, NaHCO<sub>3</sub> 25, NaH<sub>2</sub>PO<sub>4</sub> 1, glucose 11 and CaCl<sub>2</sub> 2.5; pH 7.3) continuously bubbled with O<sub>2</sub> (95%) and CO<sub>2</sub> (5%). A Ca<sup>2+</sup> channel antagonist nifedipine (dissolved at 10 mM in ethanol and used at a final concentration of 3  $\mu\text{M}$  in control Krebs) minimized muscle contraction events. Circular smooth muscle cells were impaled with glass microelectrodes filled with 3 M KCl (70–100 M $\Omega$ ). The furosemide derivative AqF022 and the AQP agonist AqF026 were applied at

final concentration (10  $\mu$ M) with 0.01% DMSO in perfused Krebs; effects were reversed by washout with control Krebs. Transmembrane potential was measured using a high impedance amplifier (Axoclamp-2B; Axon Instruments). Electrical signals were recorded with Axoscope 9.0 data acquisition software (Axon Instruments/Molecular Devices, Union City, CA).

### Aqp1 Mice

Wild-type (*Aqp1*<sup>+/+</sup>) and knockout (*Aqp1*<sup>-/-</sup>) mice<sup>5</sup> were obtained from A.S. Verkman (University of California, San Francisco, CA). Studies were performed on sex-matched littermates aged 8–12 weeks. All animals had access to standard diet and tap water *ad libitum*. The experiments were conducted in accordance with the National Research Council Guide for the Care and Use of Laboratory Animals and approved by the ethics committee of the Université catholique de Louvain.

### Peritoneal Transport Studies and Tissue Sampling

Transport of water and solutes across the peritoneal membrane was investigated in a well established mouse model of peritoneal dialysis.<sup>16,23</sup> Changes in intraperitoneal volume over time and initial ultrafiltration rates were obtained using a fluorescent bovine serum albumin conjugate (Alexafluor555-BSA, Molecular Probe, Eugene, OR) as an indicator-dilution technique, as previously described.<sup>16,35</sup> At the end of the dwell, mice were euthanized by exsanguination and samples were processed for mRNA and protein studies.

### Real-time RT-PCR

Total RNA was extracted from peritoneum, treated with DNase I and reverse-transcribed into cDNA with iScript TM cDNA Synthesis Kit (Bio-Rad Laboratories, Hercules, CA). Changes in target genes mRNA levels were determined by relative real-time quantitative PCR with a CFX96TM Real-Time PCR Detection System using iQ TM SYBR Green Supermix (Bio-Rad). Specific primers (Supplemental Table 2) were designed using Primer3 software. The normalization factor was based on the stability of four reference genes using the program geNorm version 3.4.

### Immunoblotting

SDS-PAGE and immunoblotting were performed as described.<sup>16</sup> The membranes were blocked, incubated overnight with polyclonal rabbit anti-AQP1 antibodies (Chemicon International, Temecula, CA), washed, incubated with secondary antibodies (Dako, Glostrup, Denmark), and visualized with enhanced chemiluminescence (Amersham, Little Chalfont, UK). Membranes were stripped and reprobed with a monoclonal antibody against  $\beta$ -actin (Sigma, St. Louis, MO). Densitometry analyses were performed using NIH-Image V1–57 software.

### Tissue Staining and Immunohistochemistry

Tissue samples were fixed in 4% paraformaldehyde and embedded in paraffin. Staining (hemalun-eosine and Sirius red) and immunostaining were performed as previously described.<sup>16</sup> Oocytes were fixed on day 2 or 3 after cRNA injection in 4% paraformaldehyde, permeabilized for 1 hour with 0.1% Triton X-100, and incubated with rabbit polyclonal antibody against the carboxyl terminal domain of hAQP1 (kindly provided by WD Stamer, University of Arizona). Labeling was visualized with FITC-conjugated goat antirabbit antibody and imaged with a Leica TCS-4D laser scanning confocal microscope (Nussloch, Germany).

### Transmission Electron Microscopy

Mouse peritoneum was processed for ultrastructural studies and immunogold labeling as previously reported.<sup>16</sup> Sections were incubated with rabbit anti-AQP1 antibodies, followed by protein-A gold antirabbit antibody, and viewed using a Tecnai-12 microscope (FEI, Eindhoven). The number of particles per unit length of capillary was measured using the IMOD software.

### Statistical Analyses

Data are given as mean  $\pm$  SEM. Statistical significance was evaluated by one- or two-way ANOVA followed by *post hoc* Bonferroni tests, unless otherwise indicated.

Additional methods for *in vitro* assays, AqF026 synthesis, peritoneal transport, volume curves, and calculation of initial ultrafiltration rates, and immunoelectron microscopy are provided in the Supplemental Information.

### ACKNOWLEDGMENTS

The expert assistance of H. Debaix, S. Terryn, S. Druart, J. Meissner, and L. O'Carroll is appreciated. We wish to thank Professor B. Rippe and Dr. J. K. Leyboldt for fruitful discussions and personal communications.

These studies were supported in part by the Fondation Saint-Luc at UCL, a Baxter Extramural Grant, an Action de Recherche Concertée (ARC, Communauté Française de Belgique), the Fonds National de la Recherche Scientifique, the Inter-University Attraction Pole (IUAP, Belgium Federal Government), the NCCR Kidney.CH program (Swiss National Science Foundation), and the Adelaide Centre for Neuroscience Research (AJY).

### DISCLOSURES

None.

### REFERENCES

- Agre P: Aquaporin water channels (Nobel Lecture). *Angew Chem Int Ed Engl* 43: 4278–4290, 2004
- Fu D, Lu M: The structural basis of water permeation and proton exclusion in aquaporins. *Mol Membr Biol* 24: 366–374, 2007
- Nielsen S, Smith BL, Christensen EI, Agre P: Distribution of the aquaporin CHIP in secretory and resorptive epithelia and capillary endothelia. *Proc Natl Acad Sci U S A* 90: 7275–7279, 1993
- Devuyst O, Nielsen S, Cosyns JP, Smith BL, Agre P, Squifflet JP, Pouthier D, Goffin E: Aquaporin-1 and endothelial nitric oxide synthase expression in capillary endothelia of human peritoneum. *Am J Physiol* 275: H234–H242, 1998
- Ma T, Yang B, Gillespie A, Carlson EJ, Epstein CJ, Verkman AS: Severely impaired urinary concentrating ability in transgenic mice lacking aquaporin-1 water channels. *J Biol Chem* 273: 4296–4299, 1998
- King LS, Choi M, Fernandez PC, Cartron JP, Agre P: Defective urinary-concentrating ability due to a complete deficiency of aquaporin-1. *N Engl J Med* 345: 175–179, 2001
- Verkman AS: Aquaporins in clinical medicine. *Annu Rev Med* 63: 303–316, 2012
- Stoenoiu MS, Ni J, Verkaeren C, Debaix H, Jonas JC, Lameire N, Verbavatz JM, Devuyst O: Corticosteroids induce expression of aquaporin-1 and increase transcellular water transport in rat peritoneum. *J Am Soc Nephrol* 14: 555–565, 2003

9. Gao J, Wang X, Chang Y, Zhang J, Song Q, Yu H, Li X: Acetazolamide inhibits osmotic water permeability by interaction with aquaporin-1. *Anal Biochem* 350: 165–170, 2006
10. Huber VJ, Tsujita M, Kwee IL, Nakada T: Inhibition of aquaporin 4 by antiepileptic drugs. *Bioorg Med Chem* 17: 418–424, 2009
11. Migliati E, Meurice N, DuBois P, Fang JS, Somasekharan S, Beckett E, Flynn G, Yool AJ: Inhibition of aquaporin-1 and aquaporin-4 water permeability by a derivative of the loop diuretic bumetanide acting at an internal pore-occluding binding site. *Mol Pharmacol* 76: 105–112, 2009
12. Yang B, Zhang H, Verkman AS: Lack of aquaporin-4 water transport inhibition by antiepileptics and arylsulfonamides. *Bioorg Med Chem* 16: 7489–7493, 2008
13. Devuyst O, Margetts PJ, Topley N: The pathophysiology of the peritoneal membrane. *J Am Soc Nephrol* 21: 1077–1085, 2010
14. Brimble KS, Walker M, Margetts PJ, Kundhal KK, Rabbat CG: Meta-analysis: Peritoneal membrane transport, mortality, and technique failure in peritoneal dialysis. *J Am Soc Nephrol* 17: 2591–2598, 2006
15. Yang B, Folkesson HG, Yang J, Matthay MA, Ma T, Verkman AS: Reduced osmotic water permeability of the peritoneal barrier in aquaporin-1 knockout mice. *Am J Physiol* 276: C76–C81, 1999
16. Ni J, Verbavatz JM, Rippe A, Boisdé I, Moulin P, Rippe B, Verkman AS, Devuyst O: Aquaporin-1 plays an essential role in water permeability and ultrafiltration during peritoneal dialysis. *Kidney Int* 69: 1518–1525, 2006
17. Rippe B, Stelin G, Haraldsson B: Computer simulations of peritoneal fluid transport in CAPD. *Kidney Int* 40: 315–325, 1991
18. Zelenina M, Zelenin S, Bondar AA, Brismar H, Aperia A: Water permeability of aquaporin-4 is decreased by protein kinase C and dopamine. *Am J Physiol Renal Physiol* 283: F309–F318, 2002
19. Yukutake Y, Tsuji S, Hirano Y, Adachi T, Takahashi T, Fujihara K, Agre P, Yasui M, Suematsu M: Mercury chloride decreases the water permeability of aquaporin-4-reconstituted proteoliposomes. *Biol Cell* 100: 355–363, 2008
20. Zhu MH, Kim TW, Ro S, Yan W, Ward SM, Koh SD, Sanders KM: A  $\text{Ca}^{2+}$ -activated  $\text{Cl}^{-}$  conductance in interstitial cells of Cajal linked to slow wave currents and pacemaker activity. *J Physiol* 587: 4905–4918, 2009
21. Wouters M, De Laet A, Donck LV, Delpire E, van Bogaert PP, Timmermans JP, de Kerchove d'Exaerde A, Smans K, Vanderwinden JM: Subtractive hybridization unravels a role for the ion cotransporter NKCC1 in the murine intestinal pacemaker. *Am J Physiol Gastrointest Liver Physiol* 290: G1219–G1227, 2006
22. Tomita T, Hata T: Effects of removal of  $\text{Na}^{+}$  and  $\text{Cl}^{-}$  on spontaneous electrical activity, slow wave, in the circular muscle of the guinea-pig gastric antrum. *Jpn J Physiol* 50: 469–477, 2000
23. Ni J, Cnops Y, Debaix H, Boisdé I, Verbavatz JM, Devuyst O: Functional and molecular characterization of a peritoneal dialysis model in the C57BL/6J mouse. *Kidney Int* 67: 2021–2031, 2005
24. Yool AJ, Brown EA, Flynn GA: Roles for novel pharmacological blockers of aquaporins in the treatment of brain oedema and cancer. *Clin Exp Pharmacol Physiol* 37: 403–409, 2010
25. Leeson PD, Springthorpe B: The influence of drug-like concepts on decision-making in medicinal chemistry. *Nat Rev Drug Discov* 6: 881–890, 2007
26. Yool AJ: Functional domains of aquaporin-1: keys to physiology, and targets for drug discovery. *Curr Pharm Des* 13: 3212–3221, 2007
27. Maurel C, Verdoucq L, Luu DT, Santoni V: Plant aquaporins: Membrane channels with multiple integrated functions. *Annu Rev Plant Biol* 59: 595–624, 2008
28. Yu J, Yool AJ, Schulten K, Tajkhorshid E: Mechanism of gating and ion conductivity of a possible tetrameric pore in aquaporin-1. *Structure* 14: 1411–1423, 2006
29. Törnroth-Horsefield S, Wang Y, Hedfalk K, Johanson U, Karlsson M, Tajkhorshid E, Neutze R, Kjellbom P: Structural mechanism of plant aquaporin gating. *Nature* 439: 688–694, 2006
30. Campbell EM, Birdsell DN, Yool AJ: The activity of human aquaporin 1 as a cGMP-gated cation channel is regulated by tyrosine phosphorylation in the carboxyl-terminal domain. *Mol Pharmacol* 81: 97–105, 2012
31. Smit W, Schouten N, van den Berg N, Langedijk MJ, Struijk DG, Krediet RT; Netherlands Ultrafiltration Failure Study Group: Analysis of the prevalence and causes of ultrafiltration failure during long-term peritoneal dialysis: A cross-sectional study. *Perit Dial Int* 24: 562–570, 2004
32. Musini VM, Wright JM, Bassett K, Jauca CD: Blood pressure lowering efficacy of loop diuretics for primary hypertension. *Cochrane Database Syst Rev* 4: CD003825, 2009
33. Trott O, Olson AJ: AutoDock Vina: Improving the speed and accuracy of docking with a new scoring function, efficient optimization, and multithreading. *J Comput Chem* 31: 455–461, 2010
34. Kim TW, Beckett EA, Hanna R, Koh SD, Ordög T, Ward SM, Sanders KM: Regulation of pacemaker frequency in the murine gastric antrum. *J Physiol* 538: 145–157, 2002
35. Lin YC, Samardzic H, Adamson RH, Renkin EM, Clark JF, Reed RK, Curry FR: Phosphodiesterase 4 inhibition attenuates atrial natriuretic peptide-induced vascular hyperpermeability and loss of plasma volume. *J Physiol* 589: 341–353, 2011

---

This article contains supplemental material online at <http://jasn.asnjournals.org/lookup/suppl/doi:10.1681/ASN.2012080869/-/DCSupplemental>.